Chapter 7

FABRICATION AND CHARACTERIZATION OF ALL-SPRAYED $CuInS_2/In_2S_3$ SOLAR CELL

7.1 Introduction

Photovoltaic device is probably the most suitable for the production of convenient and pollution free energy. But the major problem here is the development of easily available and eco friendly absorber that can give reasonably high efficiency cells which can produce electricity at the present cost. Recently, chalcopyrite semiconductors have been identified as absorber layers for polycrystalline thin film solar cells [1-3]. Among them, the ternary compound $CuInS_2$ (CIS) is a potential candidate due to its large absorption coefficient and optimum direct band gap of 1.5 eV, which matches well with the solar spectrum. Conversion efficiencies greater than 19% could be achieved for $Cu(In,Ga)Se_2$ (CIGS) based solar cells, using CdS as buffer layer [4]. Most of the reported studies are on development of heterojunction between p-type $CuInS_2$ and n-CdS. However, it is equally important to explore the possibility of developing a heterojunction between $CuInS_2$ and another suitable n-type wide band gap compound semiconductor, without cadmium (Cd). Now serious efforts are going on for replacing this layer by other wide band gap materials such as ZnS, ZnSe, In_xSe_y, $In_x(OH,S)_y$, In_2S_3 etc [5-9]. The motivation behind this is not only to eliminate toxic cadmium but also to improve light transmission in the blue wavelength region by using a material having band gap, wider than that of CdS.

Kazmerski et al first reported fabrication of photovoltaic device using CIS [10]. They fabricated CIS based homojunction solar cell with 3.62% efficiency. Recently CIS based solar cell, with an active area efficiency of 12.5%, was fabricated by Klaer et al [11]. The technology was based on sequential process using d.c. magnetron sputtering of the metals and sulfurization in elemental sulfur vapor. K. Siemer et al obtained efficiency of 11.4% by using rapid thermal process for the

preparation of CIS absorbers [12]. Cells having copper rich CIS phase, prepared using thermal evaporation method, could achieve efficiency of 10.2% [13]. All these cells were found to have CdS as buffer layer, deposited using Chemical Bath Deposition (CBD) technique.

Indium sulfide had already been studied as buffer layer for CIGS or CIS based solar cells [14-17]. Hariskos et al [8] achieved conversion efficiency of 15.7% using cadmium free In_x (OH, S) $_y$ buffer layer for CIGS based solar cells. Here also the buffer layer was deposited using CBD technique. Fabrication of 11.4% efficient thin film solar cell based on $CuInS_2$, with the same buffer layer, was reported by Braunger et al [18]. Efficiencies upto 14.9% for CIGS based laboratory cells, with indium sulfide buffer layer deposited using ALCVD, was reported by Spiering et al [9]. Rapid Thermal Process (RTP) for $CuInS_2$ absorber layer was found to be suitable to enhance efficiency of the cell [19]. Solar cells having superstrate configuration ZnO/CdS/ $CuInS_2$ were prepared using Chemical Spray Pyrolysis (CSP) technique by Mere et al [20].

This chapter describes fabrication and characterization $CuInS_2$ based solar cell with Cd-free β-In_2S_3 buffer layer using CSP technique. This technique is quite suitable for solar cell production because of the possibility of large area deposition of thin films at low cost with controlled dopant profiles. It is easy to vary the stoichiometric composition as well as doping profile along the thickness of the sample and multi layer films with large area could be deposited. Moreover many of the thin film solar cells have one of the electrodes to be transparent conducting oxide. This layer could be conveniently deposited using CSP technique. Hence if we adopt CSP technique for cell fabrication, almost all the layers (except top metal electrode) could be deposited using this simple technique without a break. This is very convenient for large-scale production. Preliminary results of the $CuInS_2/In_2S_3$ solar cell fabrication and characterization are given here.

7.2 Device Fabrication

7.2.1 Back Contact (ITO)

Several types of transparent conducting oxides (TCOs) are commercially produced to be used as front/back contact of solar cells. The most common TCOs are tin oxide (SnO_2), doped tin oxide such as SnO_2: F, indium tin oxide (ITO) and sometimes a combination of a tin oxide layer and indium tin oxide (ITO/SnO_2) layer. Typically, these films should have low resistance, high optical transmission and should be thermally stable during the subsequent processing steps of cell fabrication. In the present work, we used commercially available ITO films as the bottom electrode for fabricating the cell. We also used spray pyrolysed SnO_2: F, but the performance of the cells fabricated using this film as electrode was rather poor and hence the use of SnO_2: F was discarded for the present work.

Fig.7.1 shows transmission spectrum of ITO films we used. The ITO layer was 1500 Å thick, having optical transmission around 82% and electrical resistivity 2.25×10^{-4} Ω-cm. Structural analysis of the film was done using XRD and is given in Fig.7.2. The corresponding *d* values are listed in Table 7.1.

Table 7.1 XRD analysis of ITO film

2θ (degrees)	d [Å] (observed)	d [Å] (standard)	hkl
21.45	4.1400	4.1770	211
30.20	2.9570	2.9470	222
35.30	2.5406	2.5371	400
50.75	1.7975	1.7880	440
60.42	1.5310	1.5250	622

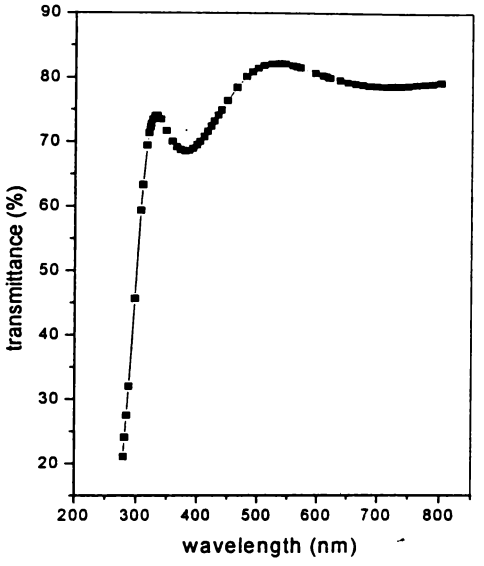

Fig. 7.1 Transmission spectrum of ITO

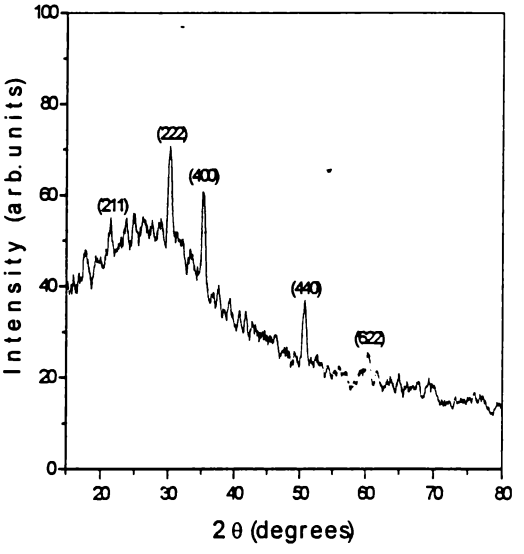

Fig. 7.2 XRD spectrum of ITO

7.2.2 $CuInS_2$ Absorber Layer

We deposited CIS layer first on the ITO surface using CSP technique. We had done extensive studies for the optimization of deposition condition of CIS using this technique and also for the characterization of the film using different techniques. Details of these studies are given in chapters 5 and 6. Hence the details of film deposition and characterization are not repeated here. We include, only a brief description of preparation conditions of junction alone. $CuInS_2$ thin films were deposited using aqueous solution containing copper chloride ($CuCl_2.2H_2O$), indium chloride ($InCl_3$), and thiourea ($CS(NH_2)_2$). Total volume of the solution sprayed was 375 ml with the following composition $CuCl_2.2H_2O$ - 0.0125 M (125 ml), $InCl_3$ – 0.0125 M (125 ml) and $CS(NH_2)_2$ – 0.0625 M (125 ml) for Cu/In ratio 1 and S/Cu ratio 5. The substrate was kept at 300 ± 5°C and the spray rate at 20 ml/min. Cu/In, S/Cu and In/S ratios of the films were controlled by varying molar concentrations of the respective compounds in the solutions. Absorber layer was found to have a tetragonal structure with preferential orientation along (112) plane. XRD spectrum of the absorber layer is given in Fig. 5.1. The band gap was found to be 1.4 eV [Fig.5.6].

7.2.3 In_2S_3 Buffer Layer

A detailed description on preparation and characterization of In_2S_3 films is given in an elaborate manner in chapter 3. Here we included only the essential aspects of preparation condition of the film deposited for junction fabrication only. In_2S_3 film was deposited over $CuInS_2$ film as buffer layer. Aqueous solution of indium chloride ($InCl_3$) and thiourea was used to deposit In_2S_3 films. For the fabrication of the solar cells we used In/S ratio 1.2/8 as it was giving maximum photosensitivity [Fig. 3.30]. For this the molarity of $InCl_3$ was kept at 0.015 M and that of thiourea at 0.1 M. XRD pattern of β-In_2S_3 buffer layer is given in Fig. 3.24. Band gap was found to be 2.65 eV, wider than that of CdS (2.4 eV) [Fig. 3.27]. Fig. 3.28 depicts the trasmission spectrum of In_2S_3 film.

7.2.4 Electrode Deposition

We deposited Aluminium as the top electrode using Physical Vapour Deposition (PVD). The grain size of the samples being small (grain size of $CuInS_2$ is ~ 10 nm [Fig. 5.1] and grain size of In_2S_3 is ~ 14 nm [Fig.3.24], the grid or comb structure of the electrodes will result in the loss of photogenerated carriers collected at the electrode. Hence we have given the electrode as a square block having area 0.04 cm^2 and thickness 50 nm. Thus this structure of the electrode had to be selected due to the low grain size of the absorber and buffer layers and this was a limitation of CSP technique. But considering other advantages of this deposition technique, we accepted it for cell deposition, we decided to have the present electrode structure for the cells. Indium was also given as the top electrode, but it always resulted in the shorting of the bilayer structure. The structure of the cell fabricated is shown schematically in Fig.7.3.

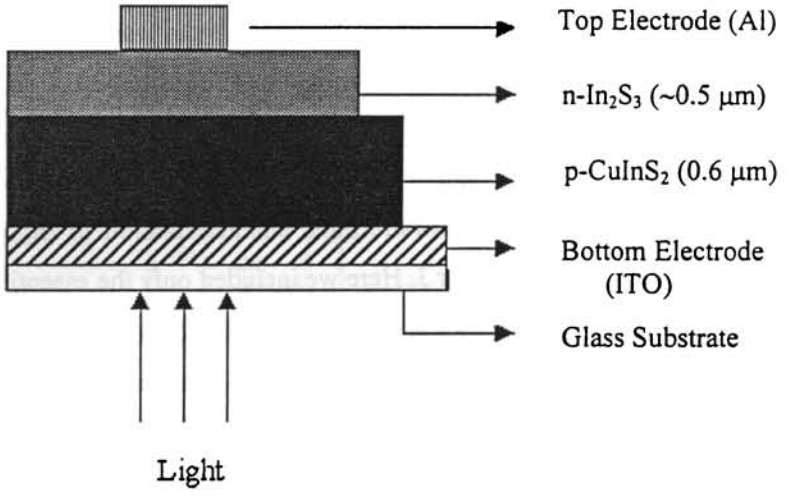

Fig. 7.3 Schematic diagram of the structure of the solar cell

7.3 J-V Characteristics of the Cell

Dark and illuminated J-V characteristics of the cell were measured using Keithley Source Measure Unit (SMU, K 236) and Metric's Interactive Characterization Software (ICS). The cell was illuminated using a tungsten halogen lamp having intensity 100 mW/cm^2 on the substrate surface. An infrared filter along with water jacket was used to remove heat content from the incident light to ensure that there was no heating of the cell during measurement. Input power was measured using a "suryamapi" (A-136 model of CEL). Distance between the cell and the source was 8 cm.

In the present work, we illuminated the junction through the substrate side. This was because of the structure of electrode. As stated earlier, electrode was deposited as a patch over In_2S_3 and hence illumination could not be given through the window layer. As the illumination was through absorber side, we wanted to make sure that enough intensity was reaching the junction region; we measured transmitted intensity on the In_2S_3 side. We found that transmitted intensity was ~ 20 mW/cm^2 even when the thickness of absorber layer was increased to 0.6 μm. This proved that enough intensity was reaching the junction region and hence there was no problem due to the illumination from absorber side. But transmission of about one fifth of the incident power unabsorbed was really undesirable and this could be a reason for low short circuit current.

Series resistance (R_s) of the cell could be calculated from the dark J-V characteristics of the cell. Inverse of the slope of far forward characteristics (in the first quadrant), where J-V becomes linear gives R_s [21]. Cell parameters V_{oc}, J_{sc} could be noted from the J-V curve and Fill Factor (FF) and efficiency (η) could be calculated using the corresponding equations. The slope of the ln J versus V graph gave diode quality factor (A) [22].

7.4 Results and Discussion

Effects of variation of atomic concentration as well as thickness of both absorber and buffer layers, on the electrical properties of the cell were studied. In all cases cells gave fairly good open circuit voltage, but low short circuit current and fill factor. Low value of fill factor might be due to the high series resistance of the sample. The presence of interface states causing trapping of photogenerated carriers might be the reason for lower value of short circuit current density. In the following sections we discuss effect of variation of important parameters like buffer/absorber layer thickness, atomic concentration etc on cell performance.

7.4.1 Effect of Having 'Superstrate' Structure

In the 'superstrate' structure the cell should have ITO/In_2S_3/$CuInS_2$/metal electrode and illumination should be given through ITO. Due to the limitation in the structure of the top electrode, we fabricated superstrate structure first. Here thickness and stoichiometry of both the layers were varied. Usually thickness of the buffer layer should be very low (~ 50 nm) in both substrate and superstrate configurations, in order to transmit maximum light to the absorber layer. We varied the thickness of In_2S_3 layer from 1 to 4 μm. At still lower thickness (<1 μm) spraying of CIS resulted in porous In_2S_3. But thicker In_2S_3 layer resulted in inactive junction even on illumination. From the XPS analysis we found that the diffusion of Cu was much prominent in the superstrate structure [Fig. 7.4]. Also, much light will get absorbed in the thick In_2S_3 layer itself, without reaching the junction region. In another set of experiments we varied the Cu/In ratio of CIS keeping S/Cu ratio at 5. This also produced no effect on illuminating the cell. But on the other hand ITO/$CuInS_2$/In_2S_3/metal electrode clearly exhibited photovoltaic action on illumination. Moreover the dark J-V characteristic was also proving the action of *pn* junction. Hence here we had ITO/$CuInS_2$/In_2S_3/metal electrode structure and illumination was through $CuInS_2$ layer. This will be clear through the studies in the following sections.

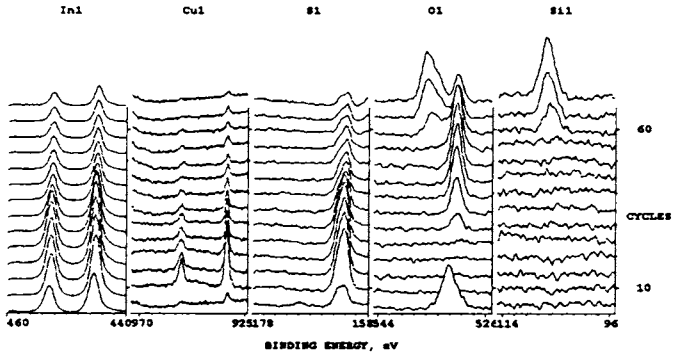

Fig. 7.4 Depth profile of the superstrate structure

7.4.2 Effect of Layer Thickness Variation

375 ml of the solution was sprayed to get ~ 0.6 μm thickness of the CIS absorber layer. In the case of In_2S_3 layer, we could get thickness of ~ 0.5 μm by spraying 200 ml of the solution. Buffer layer thickness was varied between 0.5 μm and 0.25 μm by varying the volume of the solution sprayed. For $CuInS_2$ layer, Cu/In ratio was kept at 1 and S/Cu ratio at 5 and In/S ratio at 1.2/8 for In_2S_3 layer.

On decreasing buffer layer thickness, open circuit voltage was decreased while short circuit current density increased. Variation of the cell parameters with variation in the buffer layer thickness is listed in Table 7.1. This indicated that the buffer layer had strong influence on cell parameters even when illumination was from absorber side. As thickness decreased better carrier collection might be taking place at electrode. The dark and illuminated J-V characteristics of the cell with efficiency 0.104% is shown in Fig. 7.5 (a) and (b).

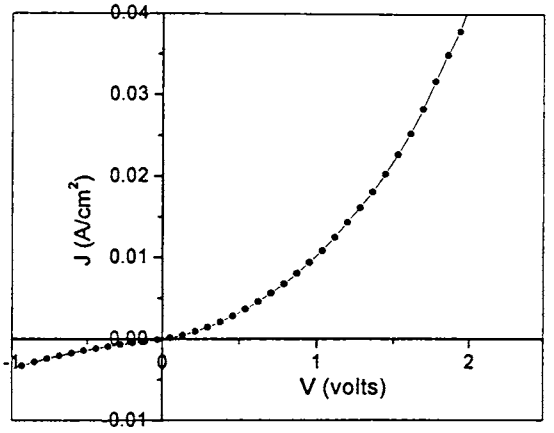

(a)

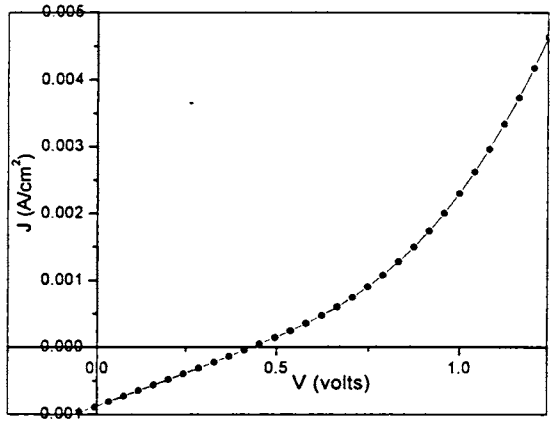

(b)

Fig. 7.5 J-V characteristics of the cell with buffer layer having 0.25 μm thickness (a) dark (b) illuminated

Table 7.1 Variation of cell parameters with thickness of the buffer layer

Thickness of $CuInS_2$ absorber layer ~ 0.6 μm (375 ml of solution)

Volume of the solution (ml)	Thickness (approx) (μm)	V_{oc} (mV)	J_{sc} (mA/cm^2)	FF (%)	η (%)
200	0.50	529.9	0.163	23.18	0.02
150	0.37	520.08	0.416	24.15	0.052
100	0.25	440.04	0.896	26.44	0.104

Keeping the thickness of the buffer layer at ~ 0.5 μm, absorber layer thickness was varied between 0.6 μm and 0.4 μm. Voltage and current density of the cell increased on decreasing the thickness of the absorber layer upto a particular value. Probably lower absorber layer thickness allowed good carrier collection at the electrode. Since light came from the absorber side in this case, lower thickness might have helped higher intensity of light to reach the junction region. But on further decreasing the absorber layer thickness both the values got reduced and this might probably be due to the reduction in absorption of light in the absorber layer. Variation of cell parameters with the variation in absorber layer thickness is given in Table 7.2. The dark and illuminated characteristics of the cell with absorber layer thickness 0.5 μm is shown in Fig.7.6.

Table 7.2 Variation of cell parameters with absorber layer thickness

Thickness of In_2S_3 layer ~ 0.5 μm (200 ml of solution)

Volume of the solution (ml)	Thickness (approx) (μm)	V_{oc} (mV)	J_{sc} (mA/cm^2)	FF (%)	η (%)
375	0.6	529.9	0.163	23.18	0.02
300	0.5	586.5	0.836	27.8	0.136
270	0.4	472.3	0.17	25.4	0.024

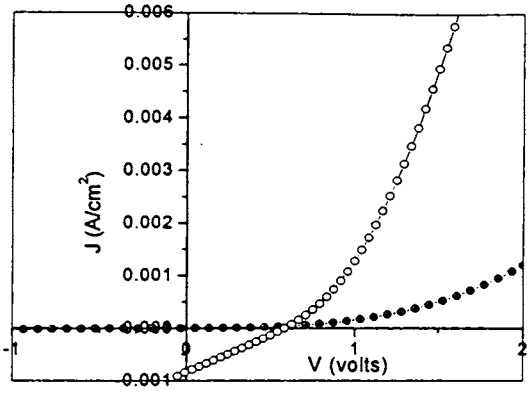

Fig.7.6 Dark and illuminated characteristics of the cell with absorber layer thickness 0.5 μm

If the value of V_{oc} is reduced by thinning the cell, then poor interface passivation is suspected [23]. The effect was clear from the XPS measurements of the cell [Fig.7.7]. There was no sharp interface between the $CuInS_2$ and In_2S_3 layer, as copper diffused into In_2S_3 layer. Copper, detected at the In_2S_3 surface was due to diffusion. This might have happened due to the high temperature (300°C) in which $CuInS_2$ film was kept, during spraying of In_2S_3 layer. Copper diffusion resulted in the formation of intermediate phases between $CuInS_2$ and In_2S_3 as well as solid mixtures of these phases. Probably this might be one of the reasons for low value of short circuit current density. Copper diffusion is an easy process, as diffusion coefficient of Cu is rather high. Studies of copper diffusion in semiconductors, particularly in $CuInSe_2$, indicated its high diffusivity [24]. Diffusion of other elements (eg. In) can also occur but the diffusion coefficient is low. Grain boundary diffusion coefficients are generally much higher that of lattice diffusion, and hence copper may be diffusing mainly through grain boundaries [25]. In fact grain boundaries are very efficient diffusion paths. Depth profile and atomic concentration of the cell CIS/IS (Cu/In = 1, S/Cu = 5, ~ 0.6 μm and In/S = 1.2/8, ~ 0.5 μm) are depicted in Fig.7.7 and 7.8. It was

evident from the XPS analysis that oxygen was present in CIS and In_2S_3 layers, probably a higher percentage of oxygen in In_2S_3 layer.

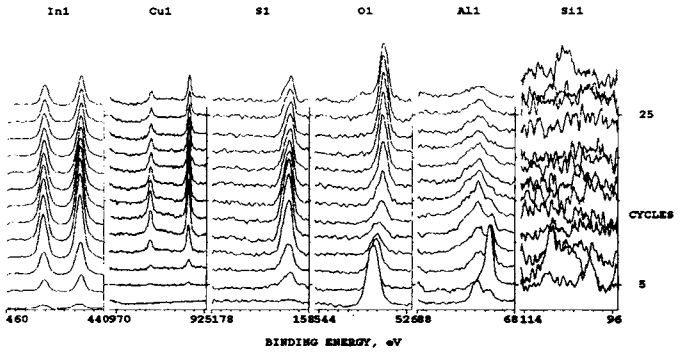

Fig.7.7 Depth analysis of the CIS/In_2S_3 cell

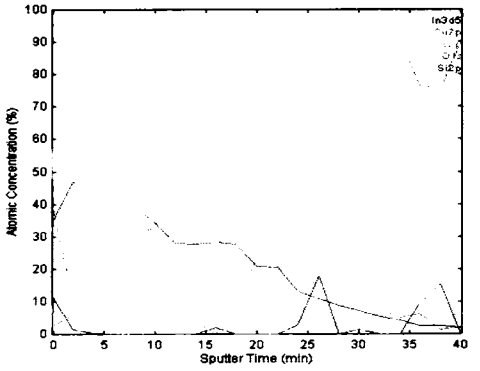

Fig. 7.8 Atomic concentration along the depth of the cell

Oxygen was present throughout the depth of the In_2S_3 layer when sprayed over $CuInS_2$ layer. Interestingly there was no oxygen in the bulk of the In_2S_3 sample when it was sprayed alone [Fig.3.25]. Since oxygen is more electronegative (3.5) than sulfur (2.4), presence of oxygen may be the reason for high resistance of In_2S_3. This might have affected electrical resistivity of the two layers and hence the short circuit current.

For 0.5 μm thickness of the absorber layer (300 ml solution) and 0.37 μm thickness of the buffer layer (150 ml solution) (ie, decreasing the thickness of both layers), efficiency of the cell was found to be decreasing. Cell parameters obtained were V_{oc} = 494.8 mV, J_{sc} = 0.063 mA/cm^2, FF = 22.34% and η = 0.007%.

7.4.3 Effect of Variation of Atomic Concentration

First we studied the effect of variation of atomic ratio of absorber layer. Keeping S/Cu ratio at 5, Cu/In ratio was varied as 0.8, 0.9, 1 and 1.2.In/S ratio was kept at 1.2/8 for In_2S_3 layer. Eventhough $CuInS_2$ film with Cu/In ratio 0.5 yielded maximum photosensitivity [Fig.5.8] it was showing n-type conductivity and thus could not be used while fabricating the cell.375 ml of the solution was sprayed to get 0.6 μm thick absorber layer and 200 ml solution was sprayed for 0.5 μm thick In_2S_3 layer. The cell having Cu/In ratio 1.2 produced maximum current density (2.5 mA/cm^2) but the voltage (405 mV) was slightly low. As the Cu/In ratio increased the dark resistivity decreased and thus more photogenerated carriers might be reaching the electrode contributing to increase in short circuit current. But increase in Cu/In ratio led to higher diffusion of Cu making junction more imperfect. This might be the reason for decrease in open circuit voltage. Efficiency decreased with decrease in Cu/In ratio. Indium rich $CuInS_2$ films had much lower hole concentration or the p-type nature of the film decreased. Enhancement of hole concentration is essential for higher efficiency of $CuInS_2$ based solar cells [26]. On increasing the sulfur concentration (S/Cu = 7) keeping the Cu/In ratio at 1, V_{oc} reduced while J_{sc} enhanced.

Increasing the sulfur concentration might be resulted in the reduction of sulfur vacancies and thus decrease recombination within the absorber layer [11]. Table 7.3 and 7.4 show variation of cell parameters with the Cu/In and S/Cu ratio of $CuInS_2$ layer. Among these, Cu/In ratio at 1.2 and S/Cu ratio at 5 gave the best result. The series resistance calculated from the dark forward characteristics, was found to be 30.08 Ω.

Table 7.3 Variation of cell parameters with Cu/In ratio (S/Cu = 5)

Cu/In ratio	V_{oc} (mV)	J_{sc} (mA/cm^2)	FF (%)	η (%)
0.8	516.1	0.022	22.40	0.003
0.9	495.0	0.153	23.83	0.018
1.0	529.9	0.163	23.18	0.02
1.2	405.3	2.5	25.90	0.26

The photosensitivity of $CuInS_2$ samples decreased drastically on increasing the Cu/In ratio [Fig.5.8]. As we increased the Cu/In ratio to 1.5, we did not get any voltage or current on illumination.

Table 7.4 Variation of cell parameters with S/Cu ratio (Cu/In = 1)

S/Cu ratio	V_{oc} (mV)	J_{sc} (mA/cm^2)	FF (%)	η (%)
3	559.40	0.052	17.80	0.005
5	529.90	0.163	23.83	0.02
6	444.08	1.070	25.40	0.12
7	472.30	1.920	24.20	0.22

On further increasing the sulfur concentration, there was no appreciable shift during illumination. This might be because of the reduction in photosensitivity of the

sample [27]. On increasing the Cu/In ratio to 1.2 keeping S/Cu ratio at 7, the short circuit current density dropped to 0.41 mA/cm^2 though the open circuit voltage remained almost the same (V_{oc} = 476.9 mV).

For Cu/In ratio 1 and S/Cu ratio 7, which gave maximum efficiency among the samples for which sulfur concentration was varied, we tried variation of thicknesses of absorber and buffer layers. On reducing the buffer layer thickness to 0.37 μm, efficiency reduced drastically to 0.09%. Keeping the buffer layer thickness at 0.5 μm, when absorber layer thickness was reduced to 0.5 μm, the efficiency got still reduced. The J-V characteristics of the cell having Cu/In ratio 1 and S/Cu ratio 7 is given in Fig.7.9.

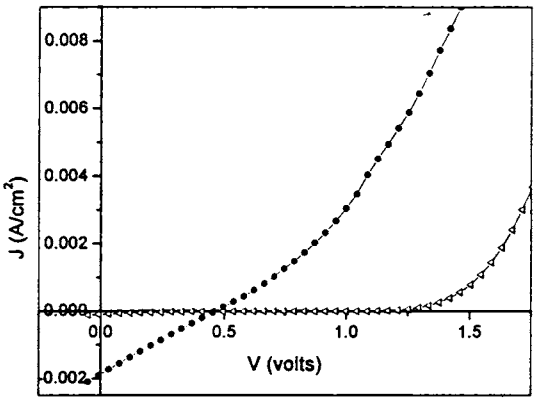

Fig. 7.9 The dark and illuminated J-V characteristics of the cell with Cu/In = 1 and S/Cu = 7

Photosensitivity of the buffer layer was found to be an important factor affecting the performance of the cell. In/S ratio was kept at 1.2/8 for the fabrication of the cells as it gave maximum photosensitivity eventhough bulk resistance of the sample was high [15]. On changing the ratio to 1.5/8 keeping the Cu/In and S/Cu ratios at 1 and 5 respectively, the current density increased while voltage decreased. This might be resulting from the reduction in resistivity of buffer layer due to increase

in indium concentration. But increasing the In/S ratio to 2/8 with the aim of reducing the series resistance of the cell produced no effect. As In/S ratio approached 2/8 resistivity might be very low affecting the survival of minority carriers. Values V_{oc}, J_{sc}, FF and efficiency are compared in Table 7.5.

Table 7.5 Variation of cell parameters with In/S ratio (Cu/In=1 and S/Cu=5)

In/S ratio	V_{oc} (mV)	J_{sc} (mA/cm^2)	FF (%)	η (%)
1.2/8	529.90	0.163	23.18	0.02
1.5/8	444.08	0.71	24	0.075
2/8	-	-	-	-

7.4.4 Effect of Post Deposition Annealing

The performance of the CIS/IS cell improved on annealing in air. Fig.7.10 shows J-V characteristics of the cell after annealing in air at 200^{0}C for 30 minutes. Value of FF improved on annealing in air (31.1%). The cell parameters obtained were V_{oc} = 528.5 mV, J_{sc} = 0.196 mA/cm^2 and η = 0.032%. Series resistance (from the dark characteristics of the cell) was found to be 19.45 Ω.

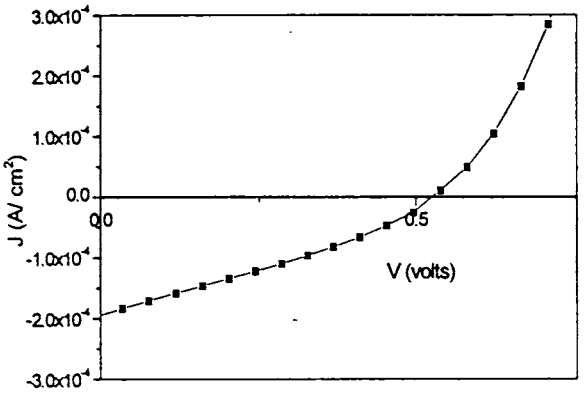

Fig. 7.10 J-V characteristics of the cell after annealing in air at 200^{0}C for 30 minutes

This was not the case with all the samples as the effect depends on the atomic concentration and the thickness of the absorber and buffer layers.

The best results were obtained when the cell was kept at the preparation temperature (300°C) itself for 1 hour, after deposition [Fig.7.11]. Cell parameters of this cell were V_{oc} = 529.7 mV, J_{sc} = 3.62 mA/cm^2, FF = 29.88% and η = 0.57%. Variation in the cell parameters after keeping the cell at the preparation temperature itself for 30 minutes, 45 minutes and 1 hour are listed in Table 7.6.

Also $CuInS_2$ layer was annealed for 1 hour after deposition before spraying In_2S_3 layer. Then the cell parameters obtained were V_{oc} = 477 mV, J_{sc} = 0.94 mA/cm^2, FF = 26.6% and η = 0.12%. On increasing the Cu/In ratio to 1.2 with S/Cu ratio 5 and 7 and keeping the cell for 1 hour after deposition at the same temperature, efficiency was found to decrease. Larger Cu/In ratio might be resulting in greater diffusion of copper from $CuInS_2$ layer to In_2S_3 layer. When the CIS/IS cell was deposited at a higher temperature (350°C), the efficiency was found to be low. This may be due to increased diffusion of Cu from CIS to In_2S_3.

Table 7.6 Variation of cell parameters with variation in the time of annealing just after depositing the cell

Cu/In = 1 S/Cu = 5, In/S = 1.2/8

Time (min)	V_{oc} (mV)	J_{sc} (mA/cm^2)	FF (%)	η (%)
30	529.9	0.163	23.18	0.02
45	559.4	2.20	23.40	0.30
60	529.7	3.62	29.88	0.57

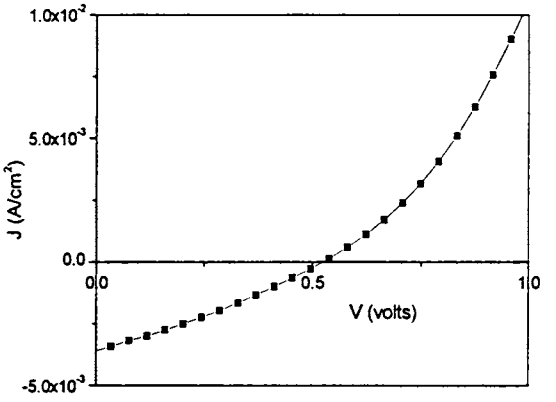

Fig. 7.11 J-V characteristics after keeping the cell at the preparation temperature (300^{0}C) itself for 1 hour, after deposition

Absorption spectrum of the cell, which was kept at the preparation temperature itself for 1 hour, is given in Fig.7.12. It showed clear absorption edges for $CuInS_2$ layer (~1.5 eV) and indium sulfide layer (~2.67 eV).

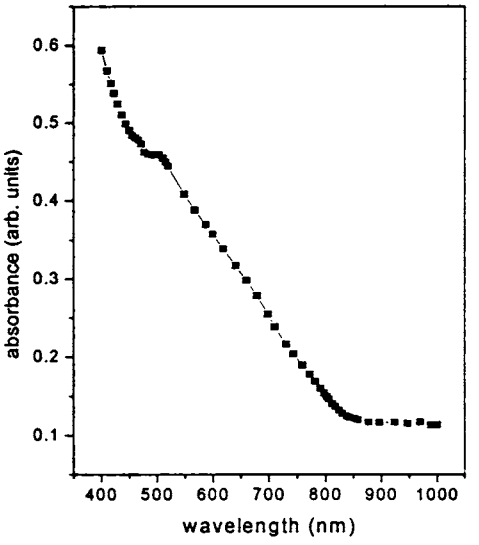

Fig. 7.12 Absorption spectrum of the best cell annealed for 1 hour

Series resistance (R_s) calculated from the inverse slope of the dark forward characteristics of the cell was 14.2 Ω. The value could also be calculated from the equation

$$R_s = \frac{1}{\lambda}\frac{1}{(I_2 - I_1)}\ln\left[\frac{I_{ph} - I_2}{I_{ph} - I_1}\right] - \left(\frac{V_2 - V_1}{I_2 - I_1}\right)$$

where, λ = q/AkT; A is diode quality factor, kT/q is thermal voltage, I_{ph} is the light generated current density, V_1, V_2, I_1 & I_2 are the voltage and current density values at any two points on the J-V characteristic curve [28].

Here $V_1 = 161.2$ mV, $I_1 = 2.75$ mA/cm^2
$V_2 = 331.3$ mV, $I_2 = 1.63$ mA/cm^2
$I_{ph} = 3.62$ mA/cm^2, A = 3.3, T = 300 K and kT/q = 0.025

Series resistance was found to be 15.18 Ω. This was in good agreement with the value obtained from the dark forward characteristics of the cell. Dark characteristics of the cell is given in Fig.7.13. Diode quality factor was calculated to be 3.3 from the slope of the dark characteristics of the cell, by plotting ln J vs V graph [Fig.7.14]. Diode quality factor >2 indicated domination of interface recombination [29], leading to reduced short circuit current density, J_{sc}. For the cells prepared using CSP technique, interface was not sharp as observed from XPS [Fig. 7.7] and this might be the reason for the low value of short circuit current density in the present work.

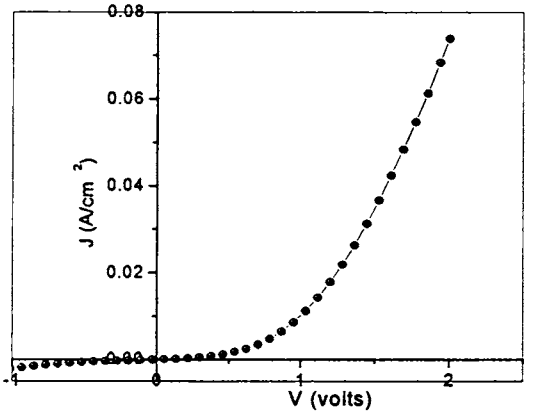

Fig. 7.13 Dark characteristics of the cell

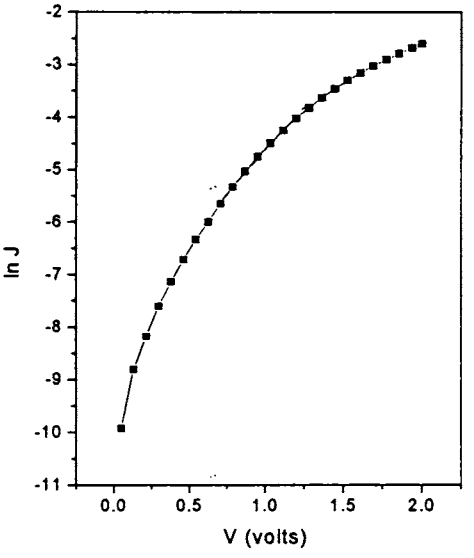

Fig. 7.14 ln J vs V graph

7.5 Conclusion

It had been shown that In_2S_3 could be used as an alternative buffer layer material for $CuInS_2$ based solar cells. It was also proved that CSP technique could be

used for deposition of both absorber and buffer layers. Again the structure of the cell was ITO/$CuInS_2$/In_2S_3/metal electrode. This structure was adopted, as we could not prepare junction in the real superstrate structure. But we found that the superstrate structure was not having junction effect at all. From XPS analysis it was clear that Cu diffused into the In_2S_3 layer, which might be the reason for low value of short circuit current density. The best cell parameters obtained were V_{oc} = 529.7 mV, J_{sc} = 3.62 mA/cm^2, FF = 29.88% and η = 0.57%. The most important step required for the improvement in the performance of the cell is the passivation of defects at the interface. However the possibility of establishment of this heterojunction using CSP technique is an encouraging result.

References

[1] J. A. M. Abushama, S. Johnston, T. Moriarty, G. Teeter, K. Ramanathan and R. Noufi *Prog. Photovolt: Res. Appl.* **12** (2004) 39

[2] M. Powalla and B. Dimmler *Thin Solid Films* **361-362** (2000) 540

[3] T. Watanabe and M. Matsui *Jpn. J. Appl. Phys.* **38** (1999) L1379

[4] K. Ramanathan, M. A. Contreras, C. L. Perkins, S. Asher, F. S. Hasoon, J. Keane, D. Young, M. Romero, W. Metzger, R. Noufi, J. Ward and A. Duda *Prog.Photovolt: Res. Appl.* **11** (2003) 225

[5] T. Nakada, M. Mizutani, Y. Hagiwara and A. Kunioka *Sol. Energy Mater. Sol. Cells* **67** (2001) 255

[6] Y. Ohtake, K. Kushiyal, M. Ichikawa, A. Yamada and M. Konagai *Jpn. J. Appl. Phys.* **37** (1998) 3220

[7] G. Gordillo and C. Calderón *Sol. Energy Mater. Sol. Cells* **77** (2003) 163

[8] D. Hariskos, M. Ruckh, U. Rühle, T. Walter, H. W. Schock, J. Hedström and L. Stolt *Sol. Energy Mater. Sol. Cells* **41/42** (1996) 345

[9] S. Spiering, D. Hariskos, M. Powalla, N. Naghavi and D. Loncot *Thin Solid Films* **431- 432** (2003) 359

[10] L. L. Kazmerski and G. A. Sanborn *J. Appl. Phys.* **48(7)** (1977) 3178

[11] J. Klaer, J. Bruns, R. Henninger, K. Siemer, R. Klenk, K. Ellmer and D. Bräunig *Semicond. Sci. Technol.* **13** (1998) 1456

[12] K. Siemer, J. Klaer, I. Luck, J. Bruns, R. Klenk and D.Bräunig *Sol. Energy Mater. Sol. Cells* **67** (2001) 159

[13] R. Scheer, T. Walter, H. W. Schock, M. L. Fearheiley and H. J. Lewerenz *Appl. Phys. Lett.* **63(24)** (1993) 3294

[14] T. Asikainen, M. Ritala and M. Leskelä *Appl. Surf. Sci.* **82/83** (1994) 122

[15] Teny Theresa John, S. Bini, Y. Kashiwaba, T. Abe, Y.Yasuhiro, C. Sudha Kartha and K. P. Vijayakumar *Semicond. Sci. Technol.* **18** (2003) 491

[16] Rupa R Pai, Teny Theresa John, Y. Kashiwaba, T. Abe, K. P. Vijayakumar and C. Sudha Kartha *J. Mat. Sci.* **39** (2004) 1

[17] Teny Theresa John, K. P. Vijayakumar, C. Sudha Kartha, T. Abe and Y. Kashiwaba *Proc. World Conference on Photovoltaic Energy Conversion (WCPEC- 3)* Osaka, Japan 1P-C3-24 (2003)

[18] D. Braunger, D. Hariskos, T. Walter and H. W. Schock *Sol. Energy Mater.Sol. Cells* **40** (1996) 97

[19] K. Siemer, J. Klaer, I. Luck, J. Bruns, R. Klenk and D. Bräunig *Sol. Energy Mater. Sol. Cells* **67** (2001) 159

[20] A. Mere, O. Kijatkina, H. Rebane, J. Krustok and M. Krunks *J. Phys. Chem. Solids* **64** (2003) 2025

[21] K. L. Chopra and S. R. Das *Thin Film Solar Cells*, Plenum Press, New York (1983)

[22] Harold J. Hovel *Semiconductors and Semimetals; Vol. II, Solar Cells*, Academic Press, New York (1975)

[23] S. R. Kurtz, J. M. Olson, D. J. Friedman, J. F. Geisz, K. A. Bertness and A. E. Kibbler *Proc. Mat. Res. Soc. Symp.* **573** (1999) 95

[24] L. Chernyak, D. Cahen, S. Zhao and D. Maneman *Appl. Phys. Lett.* **65** (1994) 427

[25] K. Djessas, S. Yapi, G. Massé, M. Ibannain and J. L. Gauffier *J. Appl. Phys.* **95(8)** (2004) 4111

[26] T. Watanabe, H. Nakazawa, M. Matsui, H. Ohbo and T. Nakada *Sol. Energy Mater. Sol. Cells* **49** (1997) 357

[27] S. Bini *Ph.D Thesis*, Department of Physics, Cochin University of Science and Technology, Kochi-682 022, India (2003)

[28] M. K. El-Adawi and I. A. Al-Nuaim *Vacuum* **64** (2001) 33

[29] M. Saad and A. Kassis *Sol. Energy Mater. Sol. Cells* **77** (2003) 415